SİDAS MEDYA
Akademik Gıda®
ISSN Online: 2148-015X
https://dergipark.org.tr/tr/pub/akademik-gida

Akademik Gıda 23(4) (2025) 256-266, DOI: 10.24323/akademik-gida.1852482

Research Paper / Araştırma Makalesi

Plasma and Chemical Deposition of Polypyrrole onto MCM-41 for Glucose Sensing

Songül Şen Gürsoy[1], Barış Balıkçı[2], Fatih Mehmet Emen[1], Abdulkerim Yıldız[2]

[1]Burdur Mehmet Akif Ersoy University, Faculty of Arts and Sciences, Department of Chemistry, TR-15200 Burdur, Türkiye
[2]Burdur Mehmet Akif Ersoy University, Institute of Applied and Natural Sciences, Department of Chemistry, TR-15200 Burdur, Türkiye

Received (Geliş Tarihi): 28.11.2025, Accepted (Kabul Tarihi): 29.12.2025
Corresponding author (Yazışmalardan Sorumlu Yazar): ssen@mehmetakif.edu.tr (S.ŞEN GÜRSOY)
+90 248 213 30 30 +90 248 213 30 99

ABSTRACT

In this study, polypyrrole/MCM-41 composite was synthesized and characterized via the two different routes of chemical and plasma methods. Glassy carbon electrodes were modified with MCM-41 and its respective composites through drop-casting, followed by drying, to be utilized in the amperometric sensing of glucose. The electrode surface was modified with glucose oxidase via cross-linking. Samples were characterized by Fourier transform infrared spectroscopy (FTIR), X-ray diffraction analysis, thermogravimetric analysis and scanning electron microscopy (SEM) techniques. The amperometric determination of glucose was achieved onto modified working electrode at +0.70V vs. Ag/AgCl. The response time of the glucose electrodes was 30 s. In fact, the electrode modified with PPy/MCM-41-plasma exhibited analytical performance comparable to that of PPy/MCM-41-chemical. However, the PPy/MCM-41-chemical composite modified electrode exhibited the superior analytical performance towards glucose compared to the pure MCM-41 and PPy/MCM-41-plasma. The upper limit of the linear working range was 4.1 mM glucose concentration for PPy/MCM-41-chemical. The glucose sensor exhibited an analytical performance, characterized by a low detection limit (LOD) of 381 nM and a high sensitivity of approximately 910.72 $\mu A.mM^{-1}.cm^{-2}$. Based on the Lineweaver-Burk plot, the sensor exhibited a K_M value of 0.009 mM, indicating a high enzymatic affinity for glucose.

Keywords: Polypyrrole, MCM-41, Glucose, Sensor, Plasma polymerization

Glikoz Sensörü Uygulaması İçin Polipirolün MCM-41 Üzerine Plazma ve Kimyasal Yöntemle Biriktirilmesi

ÖZ

Bu çalışmada, polipirrol/MCM-41 kompoziti kimyasal ve plazma yöntemleri olmak üzere iki farklı yolla sentezlenmiş ve karakterize edilmiştir. Camsı karbon elektrotlar, glukozun amperometrik tayininde kullanılmak üzere, MCM-41 ve ilgili kompozitleri ile damlatma ve ardından kurutma yöntemleriyle modifiye edilmiştir. Elektrot yüzeyi, glukoz oksidaz enziminin çapraz bağlama yöntemiyle tutuklanmasıyla modifiye edilmiştir. Numuneler; Fourier dönüşümlü kızılötesi spektroskopisi (FTIR), X-ışını kırınımı analizi (XRD), termogravimetrik analiz (TGA) ve taramalı elektron mikroskobu-enerji dağılımı X-ışını analizi (SEM-EDX) teknikleri ile karakterize edilmiştir. Glukozun amperometrik tayini, modifiye edilmiş çalışma elektrotu üzerinde Ag/AgCl referans elektrotuna karşı +0,70 V potansiyelde gerçekleştirilmiştir. Glukoz elektrotlarının yanıt süresi 30 saniye olarak belirlenmiştir. PPy/MCM-41-plazma- ile modifiye edilen elektrot, PPy/MCM-41-kimyasal ile kıyaslanabilir bir analitik performans sergilemiş olsa da; PPy/MCM-41-kimyasal kompozit modifiye elektrot, saf MCM-41 ve PPy/MCM-41-plazmaya kıyasla glukoza karşı üstün analitik performans göstermiştir. PPy/MCM-41-kimyasal için doğrusal çalışma aralığının üst sınırı 4,1 mM glukoz konsantrasyonu olarak saptanmıştır. Glukoz sensörü; 381 nM gibi düşük bir tayin sınırı (LOD) ve yaklaşık 910,72 $\mu A.mM^{-1}.cm^{-2}$'lik yüksek bir duyarlılık ile

karakterize edilen bir analitik performans sergilemiştir. Lineweaver-Burk grafiğine göre sensörün K_M değeri 0,009 mM olarak hesaplanmış olup, bu değer glukoza karşı yüksek bir enzimatik ilginin göstergesidir.

Anahtar Kelimeler: Polipirol, MCM-41, Glikoz, Sensör, Plazma polimerizasyonu

INTRODUCTION

Characterized by chronic elevations in blood glucose and subsequent metabolic irregularities, diabetes mellitus stands as one of the most critical healthcare challenges of the 21st century [1]. The global prevalence of this condition, effective control strategies are essential to minimize long-term complications affecting both small and large blood vessels, such as kidney damage and heart conditions [2]. Achieving tight glycemic control depends heavily on accurate, real-time glucose sensing, which allows clinicians and patients to make informed treatment decisions. Beyond routine maintenance, frequent testing is vital for the prevention of severe hypoglycemic events. [3]. In view of these needs, the development of high-performance glucose biosensors remains a focal point of analytical investigation. The integration of advanced nanomaterials is particularly crucial in achieving the necessary analytical metrics to ensure better clinical outcomes and patient well-being [4, 5]. The development of glucose biosensors is of paramount importance due to their diverse applications in healthcare, biotechnology, and the food industry.

Over the past years, conductive polymer materials have become a popular research area because they exhibit a lot of application areas such as polymer electrodes [6], electromagnetic interference protection [7], electrolytic capacitors [8], light emitting diodes [9], solar cells [10], chemical and biosensors [11]. Among the conducting polymers, polypyrrole (PPy) is one of the most studied polymers because of its high electrical conductivity, stability and interesting technological applications [12]. The structural uniformity of mesoporous materials makes them a prime candidate for templating the fabrication of new functional polymer composites. Conducting polymer composites with inorganic materials such as mesoporous structures have been used for inorganic and biomolecules immobilization in electroanalytical applications. MCM-41 is a type of silica with a hexagonal structure made of tiny, one-dimensional tubes (mesopores). These pores have a diameter between 2 and 10 nm [13]. Owing to its ordered pore network, large surface area, and thermal resilience, MCM-41 serves as an efficient molecular sieve for catalytic processes, chromatographic separations, and the sorption of large organic molecules, while also providing a stable environment for quantum confinement studies [14]. The synthesis and applications of several composites with conducting polymers and MCM-41 was demonstrated [15-17]. However, sensor applications of composites consisting of conducting polymers and MCM-41 remain relatively scarce in the literature [18, 19]. Furthermore, to the best of our knowledge, no prior studies have reported on the utilization of polypyrrole/MCM-41 composites specifically for glucose sensing.

In this study, efforts were made to develop a new glucose biosensor based on PPy/MCM-41 composite material. PPy/MCM-41 composite was synthesized by using plasma and chemical oxidative polymerization methods. Over the last few years, plasma polymerization has gained attention for its ability to synthesize polymer films that are difficult to produce using conventional in situ methods. A primary benefit of this approach is that the polymerization initiates in the gas phase and concludes on the nearest surface, eliminating the need for chemical oxidants. Instead, oxidation is driven by collisions between monomer molecules and free electrons accelerated by an electric field. Unlike traditional chemical synthesis, plasma-grown polymers are often free of intermediate residues but typically exhibit significant branching and crosslinking due to side reactions during growth. While such crosslinking can improve mechanical stability, it may also alter other functional properties [20]. In fact, the aim of this study is to fabricate plasma polymerized polypyrrole films on MCM-41 while preserving its semiconductor properties and to compare its usability as a glucose sensor with that of chemically synthesized films. The composites were characterized by FTIR, SEM-EDX and TGA analysis. The composite material was coated by droping and drying method on a glassy carbon electrode (GCE) used as working electrode in sensor studies. Measurements were performed in a conventional three electrode cell using a Ag/AgCl reference electrode and platinum wire as counter electrode. The use of MCM-41, PPy/MCM-41-chemical and PPy/MCM-41-plasma composites as modification materials for the development of glucose sensors was investigated. To identify the material with the optimium characteristics for glucose sensing, their responses were evaluated via chronoamperometric measurements. Furthermore, the sensor parameters were calculated and compared with previously reported glucose sensors in the literature.

MATERIALS and METHODS

Reagents and Solutions

Pyrrole (Aldrich) was purified by distillation at reduced pressure before it was used. Iron(III)chloride ($FeCl_3$), was purchased from Sigma. N-cetyltrimethylammonium bromide (CTAB), sodium hydroxide (NaOH,) Tetraethoxysilane (TEOS) were used without further purification. Double-distilled water was used for preparation of solutions. GOX (179,000 units/g) and anhydrous D-(+)-glucose served as the primary reagents for the biosensor design. Glutaraldehyde (25%) was used for crosslinking, while the supporting electrolyte was a buffer solution synthesized from sodium dihydrogen phosphate and sodium hydroxide. Alumina agglomerate (0.05 µm) was utilized for the mechanical polishing of the electrodes.

Synthesis of MCM-41

In a typical synthesis, 0.6 g of n-cetyltrimethyl-ammonium bromide (CTAB) was dissolved in 400 mL of deionized water. NaOH solution (3.5 mL of 2M) was added to the first solution, and the temperature was stabilized at 80°C. Following this, 2.5 mL of TEOS was introduced dropwise under vigorous stirring. After 2 hours of continuous agitation, the resulting white precipitate was isolated via filtration and washed thoroughly with deionized water and ethanol. Finally, the dried product was subjected to calcination at 550°C for 3 h in air to ensure the complete removal of the organic template [13] (Figure 1).

Figure 1. Mechanism of liquid-crystal templating: (1) pre-assembly of surfactant micelles and (2) the formation of a hybrid surfactant–silicate framework through organic–inorganic self-assembly

Synthesis of MCM-41/PPy Composites

Chemical Synthesis

The MCM-41 sample was dehydrated and evacuated at 200°C for 4 h to clear the channel network of residual air and water prior to use. Then, 100 mg vacuum dried powder was suspended into a pyrrole aqueous solution (for the pyrrole monomer to settle in the channels of MCM-41 by capillary effect) [15]. Then an aqueous solution of $FeCl_3$ was added to pyrrole solution. The molar ratio of $FeCl_3$ to pyrrole was maintained at 2.3.

Plasma Synthesis

Degassed MCM-41 (100 mg) was sonicated in 5 mL of ethanol for 10 min to facilitate particle dispersion. The prepared solution was spread evenly on the pre-heated glasses (5 pieces) with a pipette. The surface of MCM-41 was uniformly coated with polypyrrole via plasma polymerization. The process was carried out for 20 min in a reactor maintained at 0.30-0.35 Torr, utilizing a 13.56 MHz radio-frequency source at an output power of 40 W [20].

Preparation of Modified Electrodes

Prior to functionalization, the glassy carbon electrode (GCE) was polished to a mirror finish using a 0.05 µm alumina suspension and thoroughly rinsed with PBS. The polymer layer was prepared by dispersing 10 mg of the MCM-41, PPy/MCM-41-chemical and PPy/MCM-41-chemical in 100 µL of ethanol via ultrasonication. A 10 µL volume of this dispersion was then applied to the GCE surface using the drop-coating method. Following the evaporation of the solvent, an enzyme stock was prepared by dissolving 2.5 mg of GOx in 500 µL of PBS. To complete the biosensor fabrication, a 10 µL aliquot of this GOx solution was mixed thoroughly with 2 µL of 5% GA and applied to the modified electrode surface to ensure stable enzyme immobilization through crosslinking.

Estimation of Glucose

A 10 mL solution of 0.1 M Na_2HPO_4 buffer at an appropriate pH served as the electrolyte for the study. The response of the MCM-41, MCM-41/PPy-plasma and MCM-41/PPy chemical film-modified Glassy Carbon Electrodes (GCE) to glucose was investigated using chronoamperometry following the addition of known amounts of glucose. A three-electrode cell, equipped with separate compartments for the reference and Pt wire counter electrodes, was used for the electrochemical measurements. The solution was saturated by bubbling oxygen into the cell at a constant flow rate, which was then maintained over the solution surface to sustain saturation during the measurements. To establish the steady-state back ground current for the enzyme electrode, a potential of +0.70 V versus the Saturated Calomel Electrode (SCE) was applied. This step is essential to account for any residual current not related to the glucose-produced H_2O_2 before adding the glucose sample. Once the steady-state current value was established, known quantities of glucose were introduced into the cell from a stock solution, followed by stirring for 5 seconds. The glucose response of the electrode was measured amperometrically at a constant potential of +0.70 V against SCE, at a stirring speed of 400 rpm. This measurement quantifies the current generated by the electrooxidation of the H_2O_2 produced through the enzymatic reaction.

Glucose concentration is quantifiable via the measurement of the anodic current resulting from the oxidation of hydrogen peroxide, which is generated by the reaction detailed below.

$$\text{D-Glucose} + O_2 + H_2O \xrightarrow{\text{GOx}} \text{Gluconic Acid} + H_2O_2$$

The amperometric current measured during the oxidation of hydrogen peroxide at the electrode serves as the signal for detecting its formation:

$$H_2O_2 \rightarrow O_2 + 2H^+ + 2e^-$$

Glucose Oxidase (GOx), a type of redox protein, is utilized for the construction of the amperometric enzyme sensor. In the presence of molecular oxygen, the enzyme drives the oxidation of glucose, yielding gluconic acid and the byproduct, hydrogen peroxide. The transformation of glucose into gluconic acid is a redox process that involves the transfer of two protons ($2H^+$) and two electrons ($2e^-$) from the glucose substrate to the flavin adenine dinucleotide (FAD) cofactor, which is located in the enzyme's active site. This transfer is the key step where glucose is oxidized and the FAD cofactor is reduced ($FAD+2H^++2e^-\rightarrow FADH_2$). The subsequent reoxidation of $FADH_2$ by molecular oxygen is what ultimately produces the H_2O_2 detected by the sensor.

RESULTS and DISCUSSION

FTIR Results

Figure 2 shows five distinct curves corresponding to the MCM-41 component materials with various modifications. MCM-41 is a mesoporous silica material characterized by its ordered pore structure. Polypyrrole was incorporated into the pores of the MCM-41 to form the composite materials (PPy/MCM-41). The spectra were presented comparatively to demonstrate the presence and effect of PPy within the MCM-41 structure. Furthermore, the impact of specific treatments namely, the vacuumed state of MCM-41 and its treatment with the pyrrole monomer was also investigated by acquiring their respective spectra. The characteristic fundamental vibration bands for the silica framework of MCM-41 were observed across all spectra. Typically, the bands around 1069 cm^{-1} and 1220 cm^{-1} are attributed to the asymmetric Si-O-Si stretching vibrations. This region serves as primary evidence for the silica mesoporous structure and contains the most intense bands. The Si-OH (silanol groups) stretching vibrations observed in the 960-954 cm^{-1} range indicate silanol groups bound to the pore surface and/or defective silicon atoms on the framework. The bands observed around 810 cm^{-1} and 472 cm^{-1} correspond to the symmetric Si-O-Si stretching and bending vibrations, respectively [13, 21]. When prepared using the pelletizing technique, the Infrared (IR) spectra characteristically display two bands-a broad peak centered around 3450 cm^{-1} and a sharper one near 1640 cm^{-1} both attributed to the presence of adsorbed moisture. The widespread occurrence of these bands is owing to the intrinsic adsorption capabilities of the silanol bonds (Si-OH) present on silica and silicate surfaces [22]. The substantial reduction in bandwidth at these bands was directly attributable to dehydroxylation, which occurred as a consequence of increased the treatment temperature or vacuum applied to the samples. This reduction in band width was observed across all spectra, with the exception of the pristine MCM-41 sample. Spectroscopic analysis confirmed this change through modifications in relative band intensities and a hypsochromic shift.

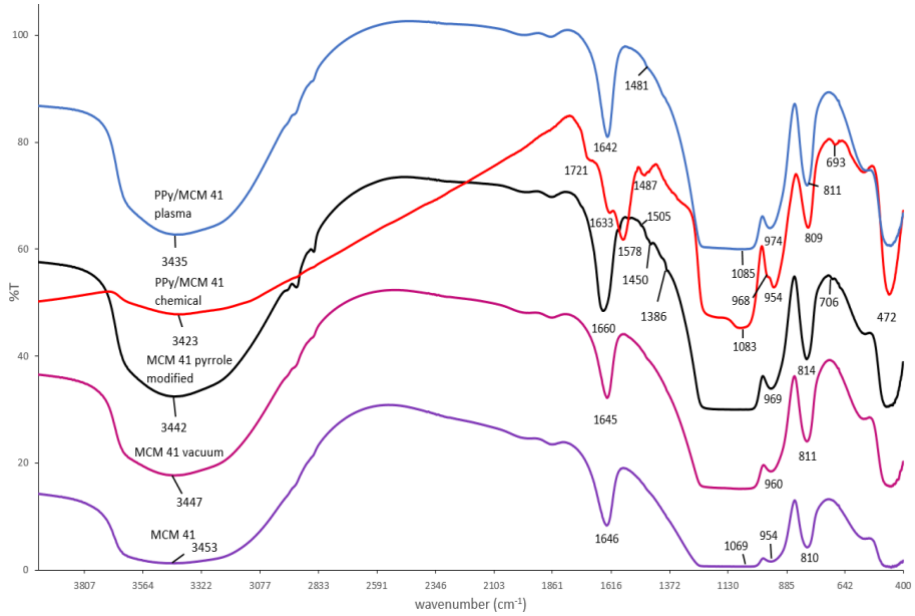

Figure 2. FTIR spectrum of samples

In the FTIR spectra of composites, new characteristic bands were observed, indicating the successful incorporation of PPy into the MCM-41 framework. In both composites, bands corresponding to C=C stretching vibrations were observed in the 1642-1505 cm^{-1} range. Additionally, C-C stretching vibrations are present in the 1487-1450 cm^{-1} range [23]. The chemically synthesized composite displayed vibrations

at 1386 cm^{-1} corresponding to C-H and N-H bending [24]. Furthermore, the bands at 1300-1000 cm^{-1} range attributed to C-H in-plane bending vibrations were observed which may overlap with the characteristic silica bands in the pyrrole-modified MCM-41 and chemically synthesized composite structures. Finally, bands attributed to C-H out-of-plane bending vibrations, observed around 974 cm^{-1}, were detected in all pyrrole-containing samples except for the pure MCM-41 samples, being most dominant in the composite synthesized via the plasma method. In the spectra of composites, particularly in the PPy/MCM-41 chemical, the intensity of this band is reduced and/or disappears. This observation strongly suggests that the Si-OH groups on the surface of the MCM-41 were coated by the pyrrole monomers during the polymerization process. This is a critical piece of evidence demonstrating that the polymer has been successfully incorporated into the MCM-41 pores and has interacted with the surface silanol groups. In the spectrum of PPy/MCM-41-chemical, the bands attributed to PPy (e.g., 1633, 1578 and 1450 cm^{-1}) appear highly intense and broad. This finding may suggest either a high polymer loading or a more amorphous polymer structure. Conversely, in the spectrum of PPy/MCM-41-plasma, the PPy bands are observed at slightly different positions (1642 and 1481 cm^{-1}) and appear sharper. This difference suggests that plasma polymerization may result in a different chemical structure or a polymer coating that is more focused on the external surface of the MCM-41.

XRD Results

The comparison X-ray Diffraction (XRD) patterns pure MCM-41 and PPy/MCM-41 chemical composite were indicated in Figure 3. Both spectra display a very broad, single reflection centered roughly between $2\theta \cong 22°$ and $2\theta \cong 25°$ [25]. This broad peak is characteristic of amorphous silica (or short-range ordered silica) and is commonly observed in the XRD patterns of pure MCM-41 at high angles [26]. This feature confirms that the basic silica frameworks of MCM-41 and the PPy/MCM-41 composite are non-crystalline or poorly crystalline [27].

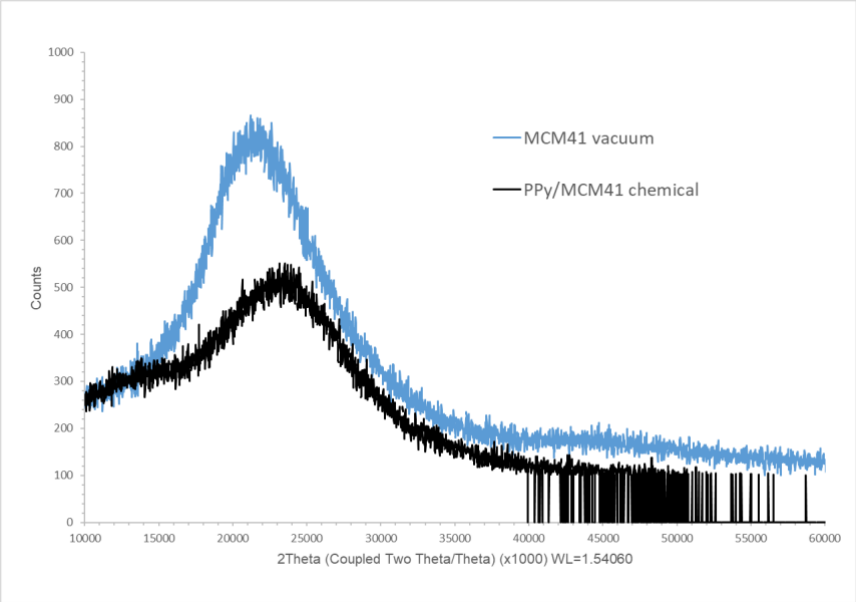

Figure 3. XRD patterns of MCM-41 and PPy/MCM-41 chemical

A comparison of the two curves reveals a significant difference in the intensity and potential broadening of the amorphous silica peak. PPy/MCM-41 chemical sample shows a lower peak intensity and appears to be broader than the MCM-41 peak. The pronounced decrease in the intensity of the characteristic silica peak in the PPy/MCM-41 composite is a strong indication of successful loading or coating of the MCM-41 pores and/or surface with PPy. The PPy polymer, which possesses a different electron density and X-ray scattering factor than silica, acts as a contrast medium, effectively reducing the coherence of the X-ray scattering from the silica wall structure. Also, the peak position also shifts slightly to a higher angle. During composite synthesis, pyrrole was first allowed to fill the pores of MCM-41, and polymerization was initiated afterwards. Therefore, the holes in MCM-41 were occupied by the polymer, leading to a change in the lattice structure. This reduced the d-spacing between atoms, resulting in an increase in X-ray diffraction and higher angles of diffraction.

SEM-EDX Results

Figure 4 (a-c) shows the SEM-EDX images of samples. SEM images of the samples indicate that the particle size of MCM-41 is at nanometer level (Figure 4a). When its composites with polypyrrole were prepared using both chemical and plasma methods, an increase in particle size was observed. The average particle sizes for both composites were around 200 nm (Figure 4b,c). This observation confirms that the surface and pores of

MCM-41 were successfully covered/filled with polypyrrole. Besides, EDX results indicate that the elemental composition of MCM-41 changes after coating with polypyrrole. Specifically, the carbon content in the PPy/MCM-41-chemical composite significantly increases (43%), whereas this increase is less pronounced in the PPy/MCM-41-plasma (34%). This value is 29% for bare MCM-41. Conversely, the silicon content exhibits a dramatic decrease in PPy/MCM-41-chemical (10%), with a lower reduction observed in PPy/MCM-41-plasma (24%). The silicon content is 32% for the bare MCM-41.

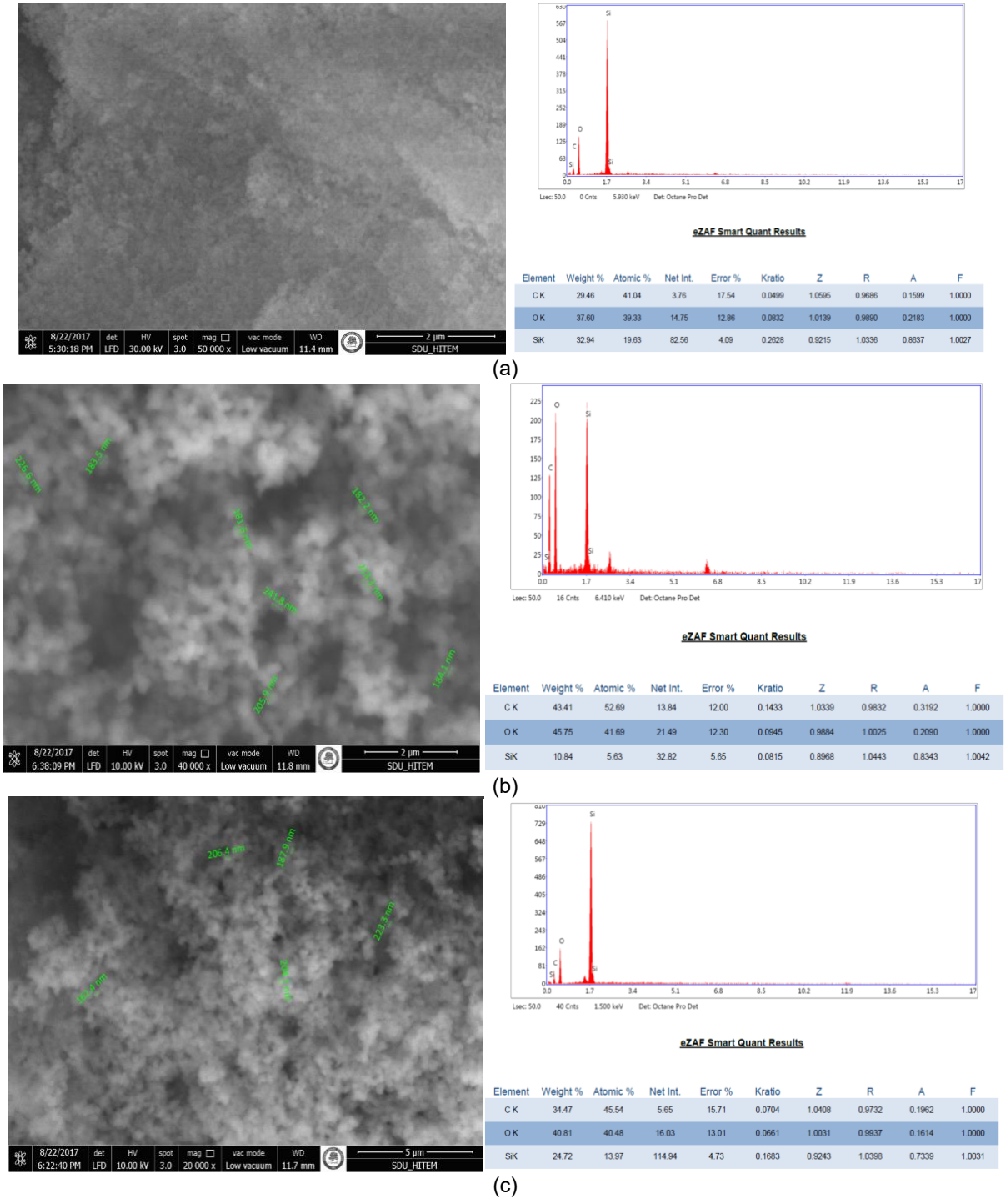

eZAF Smart Quant Results

Element	Weight %	Atomic %	Net Int.	Error %	Kratio	Z	R	A	F
C K	29.46	41.04	3.76	17.54	0.0499	1.0595	0.9686	0.1599	1.0000
O K	37.60	39.33	14.75	12.86	0.0832	1.0139	0.9890	0.2183	1.0000
SiK	32.94	19.63	82.56	4.09	0.2628	0.9215	1.0336	0.8637	1.0027

(a)

eZAF Smart Quant Results

Element	Weight %	Atomic %	Net Int.	Error %	Kratio	Z	R	A	F
C K	43.41	52.69	13.84	12.00	0.1433	1.0339	0.9832	0.3192	1.0000
O K	45.75	41.69	21.49	12.30	0.0945	0.9884	1.0025	0.2090	1.0000
SiK	10.84	5.63	32.82	5.65	0.0815	0.8968	1.0443	0.8343	1.0042

(b)

eZAF Smart Quant Results

Element	Weight %	Atomic %	Net Int.	Error %	Kratio	Z	R	A	F
C K	34.47	45.54	5.65	15.71	0.0704	1.0408	0.9732	0.1962	1.0000
O K	40.81	40.48	16.03	13.01	0.0661	1.0031	0.9937	0.1614	1.0000
SiK	24.72	13.97	114.94	4.73	0.1683	0.9243	1.0398	0.7339	1.0031

(c)

Figure 4. SEM images of MCM-41 vacuum (a), PPy/MCM-41 chemical (b), PPy/MCM-41 plasma (c).

TGA Results

The thermograms of MCM-41 and PPy/MCM-41-chemical are shown in Figure 5. MCM-41 is more resistant to temperature than PPy/MCM-41-chemical within the studied temperature range. The PPy/MCM-41-chemical has three steps of the weight loss process [15]. The first one is attributed to the removal of adsorbed water under 100°C. The second weight loss at temperatures between the range of 120 to 270°C is due

to the leaving of the dopant anion (Cl^-) from the composite structure. The third weight loss beginning at around 300°C is assigned to the decomposition of polypyrrole chains. However, the thermal stability and the percentage of residual weight (at 900°C) of the nanocomposite (60%) is enhanced significantly compared to polypyrrole (12%) synthesized in our previous study [28].

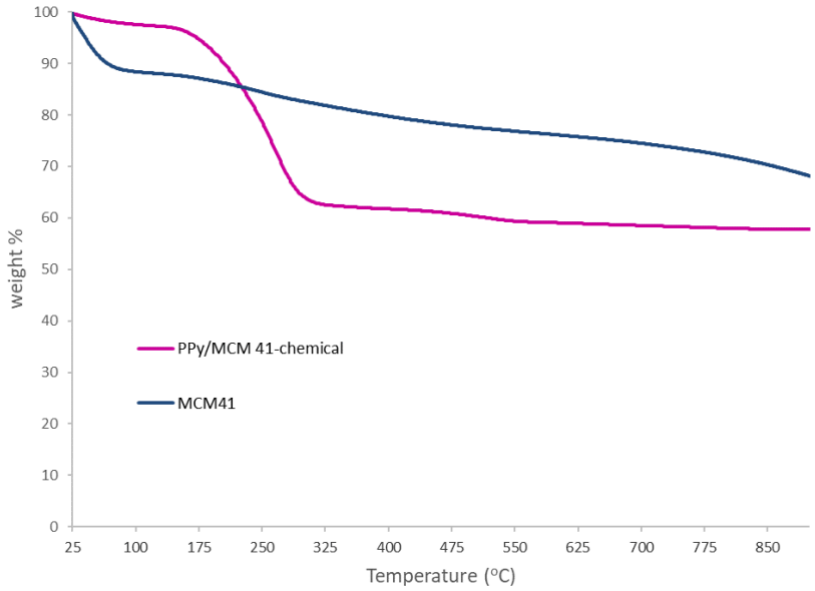

Figure 5. TGA curves of MCM-41 vacuum and PPy/MCM-41-chemical

Glucose Sensing Studies

Figure 6 indicates the amperometric curves of the samples to the addition of glucose at +0.7V. The resulting current is created by electrons passing through the system as a result of the decomposition of hydrogen peroxide, which is produced by the reaction of glucose with GOx.

At the applied potential of +0.7 V, the current response exhibits an initial increase upon glucose addition, followed by equilibration at a plateau value. The time required to reach the steady-state condition was determined to be about 30 seconds per addition.

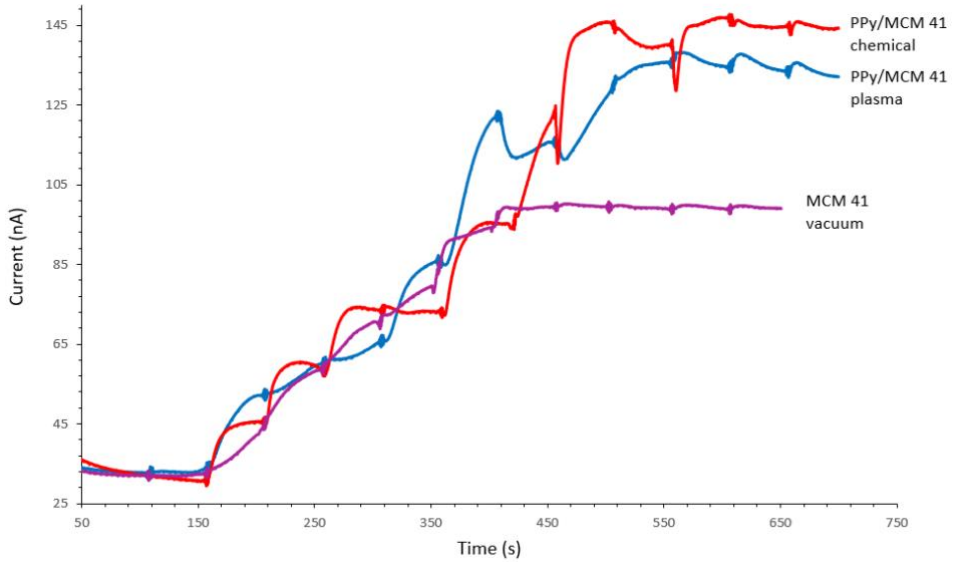

Figure 6. Amperometric response curves of MCM-41-GCE, PPy/MCM-41 plasma-GCE and PPy/MCM-41 chemical-GCE (vs. Ag/AgCl at +0,70V, PBS buffer pH 6.9, stirring speed 400 rpm, at 25°C)

Current values increased with the each addition of glucose. The obtained current values served as the data points for generating the calibration plots (Figure 7a-c).

To characterize the film kinetics, the most prevalent and simplest method was utilized: the Michaelis-Menten equation (Eq. 1). This formula is recognized as the key

chemical model for biological catalysis, from which relevant kinetic constants can be derived.

$$v = \frac{V_{\max}[S]}{K_{\mathrm{m}} + [S]} \quad [1]$$

In this equation, v represents the reaction rate, Vmax is the maximum rate, [S] is the substrate concentration, and K_M is the Michaelis-Menten constant. The Michaelis constant (K_M) serves as a critical parameter quantifying the enzyme's binding affinity for its substrate. Specifically, a lower K_M value denotes a higher affinity, meaning the enzyme requires a reduced substrate concentration to attain half of its maximum reaction velocity (Vmax/2) [29]. The maximum reaction velocity (Vmax) is indicative of the enzyme's maximal catalytic efficiency under conditions where the active sites are fully occupied by the substrate (saturation).

Among the three materials investigated for use as glucose sensors, the PPy/MCM-41-chemical composite exhibited the highest detection limit (LOD) value. However, when evaluating the performance of any enzyme sensor, the LOD value is not the sole criterion. Alongside LOD, parameters such as sensitivity, working range, maximum velocity (Vmax), and the K_M are also highly influential. Considering these aspects, the PPy/MCM-41-chemical modified electrode can be asserted to demonstrate the best overall performance.

Furthermore, a significant difference in the LOD values among the electrodes modified with these three materials is not evident. The electrode modified with PPy/MCM-41-plasma possesses performance metrics that are nearly as good as those of the PPy/MCM-41-chemical electrode. Evaluating these results, it can be concluded that preparing a composite of MCM-41 with polypyrrole (PPy) significantly enhanced the performance of the MCM-41 modified glucose sensor. Conversely, the method used for composite preparation (chemical vs. plasma) did not yield a significant difference in the final performance metrics. However, the chemical synthesis route presents disadvantages, such as a longer synthesis time compared to plasma polymerization, the requirement for an oxidizing agent, and the necessity of purification, which ultimately favor the plasma polymerization method.

The performance of the proposed glucose biosensor was compared against existing literature, specifically the titanium-containing MCM-41 (Ti-MCM-41) modified screen-printed electrodes reported by Dai et al. (2007) [30]. The sensors developed in this study exhibited superior analytical characteristics, including higher sensitivity and a lower limit of detection (LOD) than the Ti-MCM-41-SPE (5.4 $mAM^{-1}cm^{-2}$ and 0.04 mM, respectively). Furthermore, a comparison was made with the selenium nanoparticle-mesoporous silica (MCM-41) composite modified carbon paste electrode (CPE) described by Yusan et al. [31]. Under optimized conditions, their system achieved a sensitivity of 0.34 $\mu A.mM^{-1}.cm^{-2}$, an LOD of 1×10^{-4} M, and a Michaelis-Menten constant (K_M) of 0.02 mM. In contrast, our sensor demonstrates significantly enhanced sensitivity alongside lower detection limits and K_M values, indicating a higher affinity for glucose and improved overall performance.

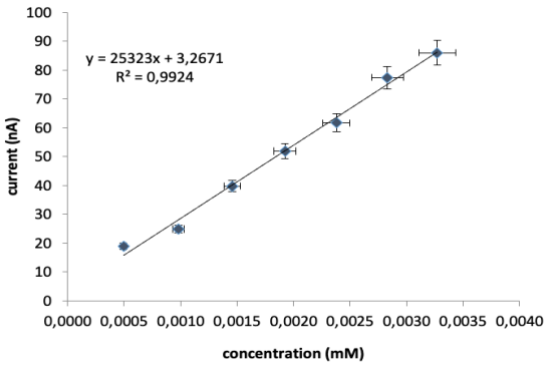

(a)

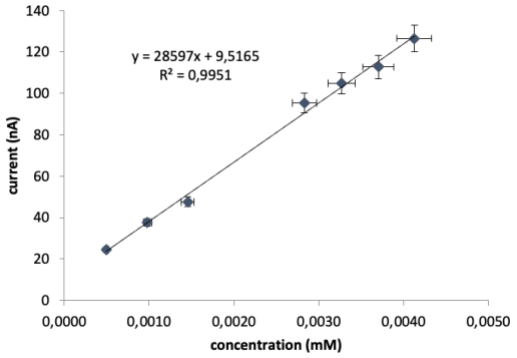

(b)

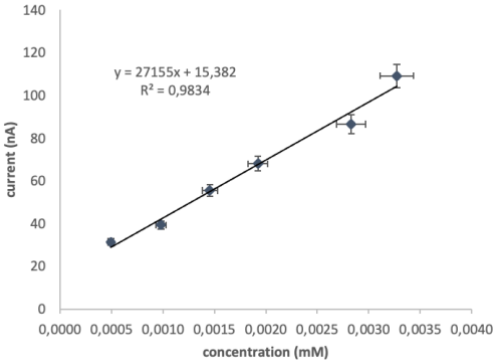

(c)

Figure 7. The calibration curve for the amperometric response of the enzyme modified electrodes (a) MCM-41-GCE (b) PPy/MCM-41 chemical-GCE, (c) PPy/MCM-41 plasma-GCE (vs. Ag/AgCl at +0,70V, PBS buffer pH 6.9, at 25°C).

In Table 1, the performance values of the developed glucose sensors were compared with that of several other glucose sensors reported in the literature. The analytical performance of the developed glucose sensors is remarkable when compared to other studies utilizing PPy and MCM-41, as presented in the table. The LOD values are lower than all other reported studies. Furthermore, the developed modified electrodes demonstrate a higher sensitivity for glucose detection than all others, with the exception of reference 35. While

the linear ranges exhibit similar characteristics, K_M values, which were not calculated in some studies, are strikingly lower in our work compared to the existing literature. In our study, the K_M value of the developed systems were lower than the previous study of us [12] for free GOx (23.53 mM). A reduced K_M suggests that mass transfer limitations (the diffusion rate of glucose to the electrode surface) have been significantly overcome or minimized by the film matrix. Besides, it shows the nondenaturating character of the procedure of enzyme anchoring [32].

Table 1. Performance values of developed glucose sensors

Sample	LOD	Sensitivity ($\mu AmM^{-1}cm^{-2}$)	Lineer range	Km (mM)	Ref.
PPy-RGO-(AuNPs-GOD)4/GCE	5.6 µM	0.89	0.2-8.0 mM	-	33
PPy/GOx/SWCNTs-$PhSO_3^-$/PB	0.01 mM	6	0.02 to 6 mM)	-	34
Ni-NPs/PPy/GRE	0.4 µM	2873	1.0-1000 µM	-	35
AuNPs-PPy-RGO	-	123.8	0.2–1.2 mM	-	36
GOx/PEI/PPy/CP	-	222.25	20–700 µM	0.36	37
(PAN-MWCNTs)/PPy	2.38 µM	81.72	0.01–2.0 mM	1.13	38
Acid-CNTs/PPy/FTO	-	95.26	10–700 µM		39
GR/Ppy-$AuNPs_{(6nm)}$ GOx/GOx	0.071 mM	55.4	up to 16.5 mmol L^{-1}	11.7	40
MCM-41	8.6 µM	467	0.2 µM-1 mM	-	41
MCM-41	0.18 mM	-	0.32 to 15.12 mM	5.2	42
MCM-41	274 nM	806.46	(0.5-3.3) mM	0.040	This study
PPy/MCM-41 chemical	381 nM	910.72	(0.5-4.1) mM	0.009	This study
PPy/MCM-41 plasma	300 nM	864.90	(0.5-3.3) mM	0.063	This study

CONCLUSION

A new glucose biosensor was developed based on a PPy/MCM-41 composite, synthesized via chemical and plasma polymerization methods. These synthesis routes were employed to integrate polypyrrole into the mesoporous silica framework for enhanced biosensing applications. FTIR spectra reveal that PPy characteristic bands emerge alongside the silica framework peaks, while the reduction of silanol signals indicates that the polymer effectively coats the internal pore surfacesusing both chemical and plasma synthesis methods. The XRD patterns verify that PPy was successfully incorporated into the MCM-41 framework. The loading is evidenced by a decrease in peak intensity and a hypsochromic shift in the amorphous silica signal, indicating that the polymer effectively occupies the mesoporous channels and interacts with the host lattice. Both chemical and plasma polymerization methods successfully encapsulated MCM-41, as evidenced by the increase in average particle size and altered elemental compositions according to the SEM-EDX studies. The decrease in silicon percentage from 32% (bare) to 10% (chemical) is a very strong indicator that the PPy layer is thick enough to attenuate the X-rays coming from the underlying silica core. This aligns perfectly with our FTIR and XRD observations. The analytical performance of the developed glucose sensors is remarkable when compared to other studies utilizing PPy and MCM-41. Evaluating these results, it can be concluded that preparing a composite of MCM-41 with polypyrrole (PPy) significantly enhanced the performance of the MCM-41 modified glucose sensor. Future efforts will focus on evaluating the proposed biosensor using real or synthetic samples. However, a comprehensive optimization of the operating parameters is required in subsequent studies. Specifically, rigorous assessments of stability, reproducibility, and interference effects must be conducted. Once these analytical performance characteristics are established, the sensor can be reliably validated for practical applications in complex matrices.

REFERENCES

[1] International Diabetes Federation. (2021). IDF Diabetes Atlas, 10th edn. Brussels, Belgium: International Diabetes Federation.

[2] American Diabetes Association. (2023). Standards of care in diabetes. *Diabetes Care*, 46 (Supplement1), S1-S4.

[3] Psoma, S.D., Kanthou, C. (2023). Wearable Insulin Biosensors for Diabetes Management: Advances and Challenges. *Biosensors (Basel).* 7;13(7), 719.

[4] Wang, J. (2008). Electrochemical glucose biosensors. *Chemical Reviews*, 108(2), 814-825.

[5] Teymourian, H., Barfidokht, A., Wang, J. (2020). Electrochemical glucose sensors in biological fluids: from kids to seniors, from pulses to continuous monitoring. *Chemical Society Reviews,* 49(21), 7671-7709.

[6] Roohi, Z., Mighri, F., Zhang, Z. (2024). Conductive polymer-based electrodes and supercapacitors: materials, electrolytes, and characterizations. *Materials,* 17(16), 4126.

[7] Zheng, S., Wang, Y., Zhu, Y., Zheng, C. (2024). Recent advances in structural design of conductive polymer composites for electromagnetic interference shielding. *Polymer Composites,* 45(1), 43-76.

[8] Romero, J.A., Azarian, M.H. Pecht, M. (2020). Life model for tantalum electrolytic capacitors with conductive polymers. *Microelectronics Reliability*, 104, 113550.

[9] Kim, Y., Nam, H., Ryu, B., Son, S.Y., Park, S.Y., Park, S., Youn, S.M., Yun, C. (2024). Thermally ınduced phase separation of the PEDOT:PSS layer for highly efficient laminated polymer light-emitting

diodes. *ACS Applied Materials & Interfaces*, 16(19) 25053-25064.

[10] Neghabi, S., Ghadari, R. (2024). Enhanced efficiency of the azo dye-sensitized solar cell via the cooperation of graphene oxide and graphene oxide/polypyrrole: Experimental and computational studies. *Electrochimica Acta*, 479, 143865.

[11] Şen Gürsoy, S., Kahraman, D. (2024). Nonenzymatic sensor based on polythiophene/titanium dioxide (PTh/TiO_2) composite for the determination of malathion in water. *Sains Malaysiana*, 53(1), 149-162.

[12] Şen Gürsoy S., Uygun A., Tilki T. (2010). Synthesis and characterization of some N-substituted polypyrrole derivatives: towards glucose sensing electrodes. *Journal of Macromolecular Science Part A- Pure and Applied Chemistry,* 47(7), 681-688.

[13] Beck, J.S., Vartuli, J.C., Roth, W.J., Leonowicz, M.E., Kresge, C.T., Schmitt, K.D., Chu, C.T.W., Olson, D.H., Sheppard, E.W., McCullen, S.B., Higgins, J.B., Schlenker, J.L. (1992). A new family of mesoporous molecular sieves prepared with liquid crystal templates. *Journal of the American Chemical Society,* 114, 10834-10843.

[14] Kato, M., Shigeno, T., Kimura, T., Kuroda, K. (2005). Synthesis of thermally stable and 2-D hexagonal super-microporous silica from hydrated α-sodium disilicate. *Chemistry of Materials,* 2005, 17, 6416-6421.

[15] Wysocka-Z˙ołopa, M., Zabłocka, I., Grądzka, E., Goclon, J., Winkler, K. (2021). Synthesis and characterization of polypyrrole@MCM-41 nanocomposites. *Microporous and Mesoporous Materials,* 317, 110954.

[16] Qi, R., Zhang, T., Guan, X., Dai, J., Liu, S., Zhao, H., Fei, T. (2020). Capacitive humidity sensors based on mesoporous silica and poly(3,4-ethylenedioxythiophene) composites. *Journal of Colloid and Interface Science*, 565, 592-600.

[17] Yang, Y., Xu, M., Jin, W. Jin, J., Dong, F., Zhang, Z., Yan, X., Shao, M., Wan, Y. (2023). PANI/MCM-41 adsorption for removal of Cr(VI) ions and its application in enhancing electrokinetic remediation of Cr(VI)-contaminated soil. *Environmental Science and Pollution Research,* 30, 121684-121701.

[18] Zablocka, I., Wysocka-Zolopa, M., Winkler, K. (2019). Electrochemical detection of dopamine at a gold electrode modified with a polypyrrole–mesoporous silica molecular sieves (MCM-48) Film. *International Journal of Molecular Sciences*, 20(1), 111.

[19] Qi, R., Lin, X., Dai, J., Zhao, H., Liu, S., Fei, T., Zhang, T. (2018). Humidity sensors based on MCM-41/polypyrrole hybrid film via in-situ polymerization. *Sensors and Actuators B: Chemical*, 277, 584-590.

[20] G.J Cruz, J Morales, R Olayo, (1999). Films obtained by plasma polymerization of pyrrole, *Thin Solid Films*, 342(1-2), 119-126

[21] Pai, P.G., Chao, S.S., Takagi, Y., Lucovsky, G. (1986). Infrared spectroscopic study of SiOx films produced by plasma enhanced chemical vapor deposition, *Journal of Vacuum Science and Technology A.* 4(3), 689–694.

[22] Eugenii, A., Paukshtis, M.A., Yaranova, I.S. Batueva, B.S.B. (2019). A FTIR study of silanol nests over mesoporous silicate materials, *Microporous and Mesoporous Materials*, 288, 109582.

[23] Kalladi, A.J., Jayan, S., Ramesan, M. T. (2024). Optical, thermal, and electrical characteristics of cashew gum/Polypyrrole/zinc oxide nanocomposites for next-gen optoelectronics. *Polymer Composites*, 45, 17030-17042.

[24] Kostic, R., Rakovic, D., Stepanyan, S.A., Davidiva, I.E., Gribov, L.A. (1995). Vibrational spectroscopy of polypyrrole, theoretical study. *Journal of Chemical Pyhsics*, 102 (8), 3104-3109.

[25] Huo, C., Ouyang, J. and Yang, H. (2014). CuO nanoparticles encapsulated inside Al-MCM-41 mesoporous materials via direct synthetic route. *Scientific Reports*, 4, 3682.

[26] Zakaria, M.B., Elmorsi, M.A., and Ebeid, El-Z.M. (2015). Corrosion protection of aluminum metal using MCM-41 films supported by silver nanoparticles and distyrylpyrazine photopolymer. *Advanced Science, Engineering and Medicine,* 7, 1-6.

[27] Tanev, P.I., Pinnavaia, T.J. (1995). A neutral templating route to mesoporous molecular sieves. *Science,* 267(5199), 865-867.

[28] Ozkan, S., Sen Gursoy, S. (2016). Pyrrole/N-p-toluenepyrrole copolymers in the presense of surfactants: A promising material for glucose sensing. *Polymer Engineering and Science,* 56(9) 995-1003.

[29] Michaelis, L., Menten, M.L. (1913). Die kinetik der invertinwirkung. *Biochemische Zeitschrift,* 49, 333-369.

[30] Yusan, S., Rahman, M.M., Mohamad, N., Arrif, T.M., Latif, A.Z.A., Mohd Aznan, M.A., Wan Nik, W.S.B. (2018). Development of an amperometric glucose biosensor based on the ımmobilization of glucose oxidase on the Se-MCM-41 mesoporous composite. *Journal of Analytical Methods in Chemistry*, 2687341, 8.

[31] Dai, Z., Fang, M., Bao, J., Wang, H., Lu, T. (2007). An amperometric glucose biosensor constructed by immobilizing glucose oxidase on titanium-containing mesoporous composite material of no. 41 modified screen-printed electrodes. *Analytica Chimica Acta*, 591(2), 195-199.

[32] Cui, L., Xu, M., Zhu, J., Ai, S. (2011). A novel hydrogen peroxide biosensor based on the specific binding of horseradish peroxidase with polymeric thiophene-3-boronic acid monolayer in hydrophilic room temperature ionic liquid. *Synthetic Metals*, 161(15-16), 1686-1690.

[33] Wu, B., Hou, S., Xue Y., Chen, Z. (2018). Electrodeposition–assisted assembled multilayer films of gold nanoparticles and glucose oxidase onto polypyrrole-reduced graphene oxidematrix and their electrocatalytic activity toward glucose. *Nanomaterials*, 8(12), 993.

[34] Raicopol, M., Prună, A., Damian, C., and Pilan, L. (2013). Functionalized single-walled carbon

nanotubes/polypyrrole composites for amperometric glucose biosensors. *Nanoscale Research Letters*, 8, 316.

[35] Emir, G., Dilgin, Yusuf., Ramanaviciene, A., Ramanavicius, A. (2021). Amperometric nonenzymatic glucose biosensor based on graphite rod electrode modified by Ni-nanoparticle/polypyrrole composite. *Microchemical Journal*, 161, 105751.

[36] Xue, K., Zhou, S., Shi, H., Feng, X., Xin, H., Song, W. (2014). A novel amperometric glucose biosensor based on ternary gold nanoparticles/polypyrrole/reduced graphene oxide nanocomposite. *Sensors and Actuators B: Chemical*, 203, 412-416.

[37] Pan, L.Y., Liu, C.H., Lai, Y.T., Lee, C.Y., Gupta, S., Tai, N.H. (2025). Fabrication of polypyrrole nano-array modified carbon paper electrodes for enzymatic salivary glucose detection. *Microchemical Journal*, 213, 113932.

[38] Çetin, M.Z., Guven, N., Apetrei, R.M., Camurlu, P. (2023). Highly sensitive detection of glucose via glucose oxidase immobilization onto conducting polymer-coated composite polyacrylonitrile nanofibers. *Enzyme and Microbial Technology*, 164, 110178.

[39] Huang, G.K., Gupta, S., Lee, C.Y., Tai, N.H. (2022). Acid-treated carbon nanotubes/polypyrrole/ fluorine-doped tin oxide electrodes with high sensitivity for saliva glucose sensing. *Diamond and Related Materials*, 129, 109385.

[40] Ramanaviciene, A., Ramanavicius, A. (2021). Dispersed conducting polymer nanocomposites with glucose oxidase and gold nanoparticles for the design of enzymatic glucose biosensors. *Polymers*, 13, 2173.

[41] Caro-Jara, N., Mundaca-Uribe, R., Zaror-Zaror, C., Carpinelli-Pavisic, J., Aranda-Bustos, M., Peña-Farfal, C. (2013). Development of a bienzymatic amperometric glucose biosensor using mesoporous silica (MCM-41) for enzyme, immobilization and its application on liquid pharmaceutical formulations. *Special Issue:14th International Conference on Electroanalysis, ESEAC 2012*, Portorož, Slovenia, 308-315.

[42] Dai, Z.H., Ni, J., Huang, X.H., Lu, G.F., Bao, J.C. (2007). Direct electrochemistry of glucose oxidase immobilized on a hexagonal mesoporous silica-MCM-41 matrix. *Bioelectrochemistry*, 70(2), 250-256.